

Articles

Simple Pyrene Derivatives as Fluorescence Sensors for TNT and RDX in Micelles

Jung-Ho Hong, Jung-Hwa Choi, and Dong-Gyu Cho*

*Department of Chemistry, Inha University, Incheon 402-751, Korea. *E-mail: dgcho@inha.ac.kr*

Received June 13, 2014, Accepted July 2, 2014

Various pyrene derivatives were synthesized and systematically examined in micelles. Synthesized mono and bispyrene derivatives were tested in micelles so that they displayed a strong excimer band and the excimer band was quenched in the presence of TNT and RDX. In the optimized condition, the binding constant for TNT of a simple dipyrene derivative **4** was increased up to $1.0 \times 10^6 \text{ M}^{-1}$ in cetyl trimethylammonium bromide (CTAB) micelles, which allowed for the detection of 2 ppb of TNT and 334 ppb of RDX by fluorescence titrations.

Key Words : Pyrene, Sensors, Fluorescence, TNT, RDX

Introduction

The rapid and sensitive analysis of nitrated explosives is in high demand for the protection of the society from terrorism as well as for controlling environmental pollution.¹ Therefore, intensive efforts have been made to develop new techniques for detecting nitrated explosives in the past decade.² However, research for obtaining new fluorophores³ and developing the related materials⁴ is still attractive because of their high sensitivity, quick response, and easy sample preparation.

In principle, efficient coupling of the π electrons on the fluorophore to the quencher (nitrated explosives) creates an exciplex, which then leads to deactivation of the fluorophore.⁵ Although 2,4,6-trinitrotoluene (TNT) and 1,3,5-trinitroperhydro-1,3,5-triazine (RDX) are representative nitrated explosives, TNT quenches fluorophores more efficiently than does RDX due to the facile formation of charge-transfer complexes. Thus, most fluorophores do not show dramatic changes in fluorescence in the presence of RDX, especially in solution. Consequently, reliable fluorescence detection for RDX in solution has proven to be challenging.

To date, few methods for detecting fluorescence signals in RDX have been reported. As an example, the Swager group have reported an impressive turn-on system for the fluorescence detection of RDX and PETN ((3-nitrooxy-2,2-bis-(nitrooxymethyl)propyl) nitrate).⁶ Their system relies on the photo-oxidation of a zinc-coordinated acridine dye to a fluorescent acridinium species in the presence of RDX or PETN. Using this method, both RDX and PETN can be detected, although TNT cannot be detected. Quantum dots with surface modification by NADH⁷ or the electron-rich 6-hydroxydopamine have also been used as alternative fluorescence dyes for detecting RDX.⁸ Along this line, our group has reported simple dipyrenyl compounds that effectively detect TNT by forming a charge-transfer complex. This

complex quenches the resulting excimer, which allows the detection of 2 ppb of TNT in semi-aqueous solution.⁹ However, in the presence of RDX, no fluorescent change in the excimer was detected. To overcome this disadvantage, we focused on the behavior of simple pyrene derivatives and nitrated explosives in micelles. Surprisingly, fluorophores are not directly used to detect nitrated explosives in micelles. Unlike our approach, the Anslyn group reported a differential array system of fluorophores that detects and identifies small nitrated analytes in Tween 80 (polyoxyethylene (20) sorbitan monolaurate) by pattern recognition.¹⁰ According to the literature, 100 mM of pyrene induces very weak excimer band ($I_{\text{ex/mo}}, I_{7,470}/I_{7,370} = \text{less than } 0.9$)¹¹ in Tween 80 (2 mM). Inferred from the literature, such a weak excimer band of simple pyrene may not be useful as the sole fluorophore for detecting nitrated explosives. Therefore, we postulate that pyrene derivatives could display a strong excimer band as they are forced to locate in micelles. Moreover, the enforced hydrophobic cavity in micelles could allow RDX to quench the excimer band of pyrene. Here, this is the first example that pyrene derivatives can detect both TNT and RDX in micelles. In particular, by screening micelles and pyrene derivatives, the binding constant of bispyrene derivative for TNT was increased up to $1.0 \times 10^6 \text{ M}^{-1}$, which allowed the detection of 2 ppb of TNT and 334 ppb of RDX by fluorescence titrations.

Experimental

Reagents were purchased at the highest commercial quality and used without further purification, unless otherwise stated. Yields of synthesized compounds were measured after chromatographic purification. UV-Vis and fluorescent spectra were recorded on UV 1800 and RF-5301 PC spectrophotometers (Shimadzu), respectively. Proton and ¹³C-NMR spectra were measured at 25 °C using a Varian Unity Innova 400

MHz instrument.

8-(Pyren-1-ylmethoxy)octan-1-ol (3). To a suspension of 1-(bromomethyl)pyrene (500 mg, 1.69 mmol) and 1,8-octanediol (160 mg, 1.09 mmol in dry DMF (10 mL) were sodium hydride (180 mg, 4.50 mmol) added at 0 °C. The reaction mixture was then stirred for 4 h at room temperature. The reaction mixture was quenched with cold water and the organic layer was extracted with dichloromethane. After the solvent was removed under reduced pressure, the residue was subjected to flash chromatography (EtOAc/hexane = 1/6) to afford **3** (244 mg, 0.68 mmol, 62.1% yield) and the known **4** (68 mg, 0.12 mmol, 10.7% yield) as yellow solids: mp 48.2–50.1 °C; ¹H NMR (400 MHz, Chloroform-*d*) δ 8.38 (d, *J* = 9.3 Hz, 1H), 8.23–8.11 (m, 4H), 8.05–7.98 (m, 4H), 5.25 (s, 1H), 5.21 (s, 2H), 3.60 (t, *J* = 6.6 Hz, 2H), 3.56 (t, *J* = 6.5 Hz, 2H), 1.69–1.19 (m, 12H); ¹³C NMR (100 MHz, CDCl₃) δ 131.92, 131.37, 131.32, 130.96, 129.45, 127.69, 127.55, 127.43, 127.02, 126.01, 125.27, 125.26, 125.05, 124.87, 124.59, 123.65, 71.60, 70.61, 63.05, 32.84, 29.94, 29.47, 26.27, 25.77; FAB: *m/z* [M]⁺ calcd for C₂₅H₂₈O₂: 360.2089; found: 360.2091.

***N,N,N*-Trimethyl-8-(pyren-1-ylmethoxy)octan-1-aminium bromide (6).** To a solution of **5** (90 mg, 0.21 mmol) in EtOH (3 mL) was added trimethylamine (418 mg, 2.13 mmol in 30% EtOH). The solution was stirred for two days. The solvent was removed under reduced pressure, and a few drops of acetone were added to initiate the formation of white solids. The white solid was filtered and washed with acetone and *n*-hexane, which afforded **6** (46.6 mg, 0.097 mmol, 45.4% yield) as a white solid: mp 160.5–163.3 °C; ¹H NMR (400 MHz, DMSO-*d*₆) δ 8.38 (d, *J* = 9.2 Hz, 1H), 8.35–8.22 (m, 4H), 8.18 (m, 2H), 8.14–8.05 (m, 2H), 5.17 (s, 2H), 3.58 (t, *J* = 6.4 Hz, 2H), 3.20 (m, 2H), 3.00 (s, 9H), 1.68–1.45 (m, 4H), 1.42–1.02 (m, 8H); ¹³C NMR (100 MHz, DMSO-*d*₆) δ 132.2, 130.7, 130.5, 130.3, 128.6, 127.4, 127.4, 127.2, 127.0, 126.3, 125.3, 125.2, 124.5, 124.0, 123.8, 123.6, 70.4, 69.6, 65.2, 52.1, 29.2, 28.5, 28.4, 25.6, 21.9; FAB: *m/z* [M]⁺ calcd for C₂₈H₃₆NO⁺: 402.2797; found: 402.2798.

Results and Discussion

To test this hypothesis, we prepared each micelle at a various concentrations of pyren-1-ylmethanol (**1**) at slightly above critical micelle concentrations (CMCs) of cetyl trimethylammonium bromide (CTAB, > 1 mM), sodium monododecyl sulfate (SDS, > 7 mM), and Tween 80 (> 0.012 mM) shown in Figure 1.¹² These micelles are representative examples of cationic, anionic, and neutral micelles, respectively. Then, the fluorescence spectra of commercially available pyren-1-ylmethanol (**1**) were monitored as the concentration of this compound increased in each micelle. Different relative excimer ratios (*I*_{ex/mo}) were observed in the three different micelles in Figure 1. While the limited solubility of **1** in Tween 80 allowed concentrations of up to 3 μM to be examined, a better excimer ratio (*I*_{ex/mo}) was observed in the cases of CTAB over the concentration range

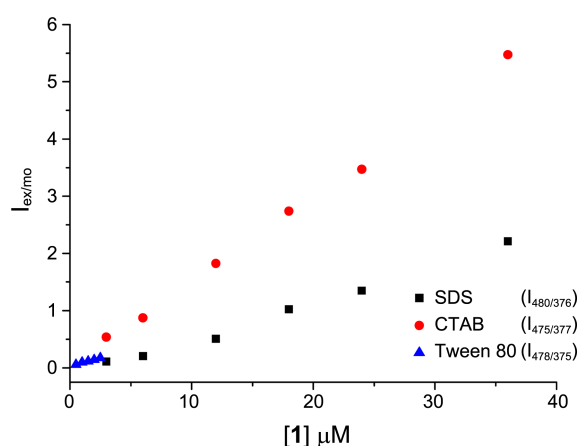
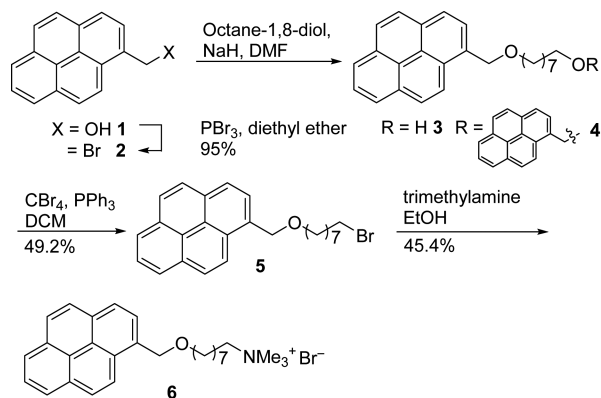


Figure 1. Relative excimer ratios (*I*_{ex/mo}) of **1** observed at the critical micelle concentrations of CTAB (1.0 mM), SDS (8.0 mM), and Tween 80 (15 μM), as the concentration of **1** increases at 25 °C. Each solution was irradiated at 345 nm.

5–40 μM. Generally, increases in the CTAB concentration resulted in higher excimer ratios. Aggregation numbers of CTAB micelles are known to range from 60 to 89 molecules; if we use 24 μM of **1** dissolved in 16.7–11.2 μM of CTAB micelle, an individual CTAB micelle contains approximately 2.1–1.4 numbers of **1**.¹² Similarly, an individual SDS micelle (62 aggregation molecules per micelle) contains 0.19 numbers of **1** (24 μM), while an individual Tween 80 micelle (60 aggregation molecules per micelle) possesses 12 numbers of **1** (3 μM).¹² These calculations, along with Figure 1, imply that the relative excimer ratio does not depend on the number of pyrene derivatives per micelle, but rather on the structure of micelle. These results partly support our hypothesis that pyrene derivative **1** can dominantly exist in dimeric forms and displays a strong excimer band in CTAB micelles.

Once CTAB was selected as a more useful micelle than the others, new pyrene derivatives based on **1** were designed and synthesized. These derivatives were designed to possess various functional groups such as alcohols, halides, and ammonium salts. We also assumed that a pyrene derivative smaller in size than CTAB (23.145 Å, optimized by semi-empirical PM3 calculation) could be easily accommodated



Scheme 1. Syntheses of fluorescence sensors for nitrated compounds.

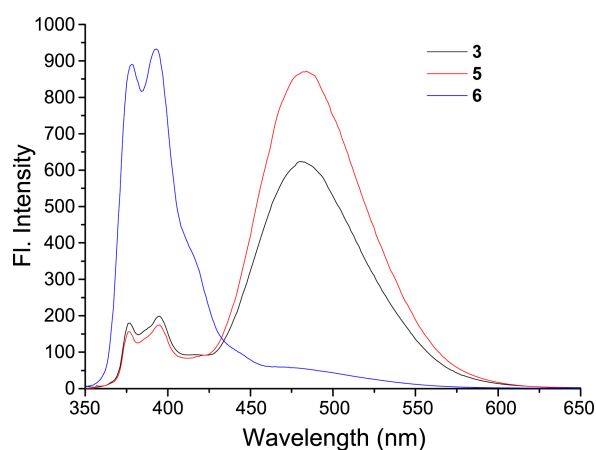


Figure 2. The fluorescence spectra of **3**, **5**, and **6** seen as irradiated at 345 nm in CTAB (1.0 mM) micelle. **3** and **6** were dissolved in only water, while **5** was dissolved in water containing 1% acetone. Each solution has 24 μM of pyrene derivative.

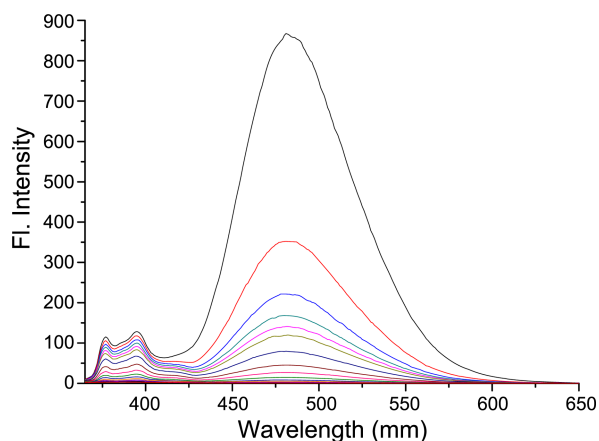


Figure 3. Evolution of the fluorescence spectrum of **5** (24 μM in water containing 1% acetone), observed during titration with trinitrotoluene (4.8 mM in DMSO, 0, 0.2 to 20 equiv.) and irradiated at 345 nm in CTAB micelle (1.0 mM).

in the CTAB core. Therefore, the molecular size was chosen to be smaller than that of CTAB. To obtain various functional group-capped compounds, 1-(bromomethyl)pyrene (**2**) was obtained by the bromination of **1**, in 95% yield. Then, **2** was reacted with 1,8-diol in the presence of NaH, which afforded the elongated alcohol **3** and dipyrenyl compound **4**⁹ in 62% and 11% yields, respectively. The elongated alcohol **4** was re-brominated with CBr_4 and PPh_3 in CH_2Cl_2 to afford the desired product in 50% yield. Bromide **5**¹³ was further modified with trimethylamine to produce the ammonium salt in 45% yield.

The synthesized chemosensors (24 μM) were tested under the optimal micelle conditions described above (1 mM CTAB in water). As shown in Figure 2, the fluorescent spectrum of **5** shows two monomeric peaks at 378 and 398 nm, and one broad excimer peak at 484 nm. Among three derivatives, the long chain bromide **5** displays the highest relative excimer ratio ($I_{481}/I_{377} = 7.5$), followed by **3** and **6**, respectively, in the CTAB solution (1 mM). This trend may

Table 1. TNT binding constants (K_a ; M^{-1})^a of chemosensors (24 μM) in CTAB (1 mM in water)^b or CTAB (1 mM in water containing 1% acetone)^c at 25 $^\circ\text{C}$

	3 ^b	5 ^c	6 ^b
TNT	9.4×10^3	2.9×10^5	1.7×10^4
RDX	6.9×10^3	1.6×10^4	1.1×10^4

^aValues were determined by fluorescence spectroscopic titrations.

be responsible for more hydrophobic nature of **5** than others. Due to the limited solubility of **5** in pure water, the micelle condition of **5** was only adjusted with 1% acetone. Upon the addition of TNT to the solution of **5** in CTAB micelle, both the monomer and excimer bands decreased (Figure 3). These changes are typically observed when excimer formation is effectively interfered. This result demonstrates that **5** mainly exists as a dimeric species in the CTAB micelle and that the predicted charge-transfer complexes can readily form where TNT is present.

The binding constants of the synthesized compounds were determined through fluorescence titrations, as summarized in Table 1. The order of affinity for TNT is $\mathbf{5} \gg \mathbf{6} > \mathbf{3}$ in the CTAB solution (1 mM) (Figures S1, S2, and S3 in ESI). The observed large binding constant of **5** may be attributed to the hydrophobic nature of **5**. As indicated above, chemosensor **5** was titrated with TNT and RDX in a 1% acetone solution. Thus, the effect of 1% acetone in the TNT titration of **5** was indirectly estimated. As each TNT titration of **3** was conducted in water containing 1% acetone or in water only, the TNT binding constants of **3** were found to be 9.4×10^3 and $7.1 \times 10^3 \text{ M}^{-1}$, respectively (Figure S1 vs. S5 in ESI). This result indicates that acetone in micelles may induce malignant effects for the TNT binding constant. In addition, the order of affinity for RDX was $\mathbf{5} > \mathbf{6} > \mathbf{3}$ under the same conditions (Figures S1, S2, and S3 in ESI). Considering the observed binding trends for TNT and RDX, hydrophobic nature of pyrene derivatives could be crucial and any reasonable explanation for the observed binding trends is something elusive in CTAB micelles.

Theoretically, this sensory system requires two molecules of pyrene derivatives in an individual micelle. Thus, bispyrene **4** could be used at a lower concentration than **5** in CTAB, since two pyrenyl groups of **4** are already present. It should be also noted that bispyrene **4** has been reported for detecting nitrated aromatic compounds in semi-aqueous solution without micelles in our group.⁹ In the previous studies, 1.55 μM of **4** was used for detecting nitrated explosives. The binding constant of **4** was $2.7 \times 10^5 \text{ M}^{-1}$ for TNT in semi-aqueous solution and the same condition provided a nearly fourfold increase as compared to that of **4** ($K_a = 1.0 \times 10^6 \text{ M}^{-1}$, Figures S4 in ESI) for TNT in CTAB micelles. Additionally, **4** displayed a reasonable binding constant for RDX in CTAB ($K_a = 6.8 \times 10^4 \text{ M}^{-1}$, Figures S4 in ESI), while no detectable binding phenomenon was observed in semi-aqueous solution. These experiments clearly show that unusual properties of **4** and **5** could be due to their enforced residence in the CTAB micelles. Moreover, the residence of

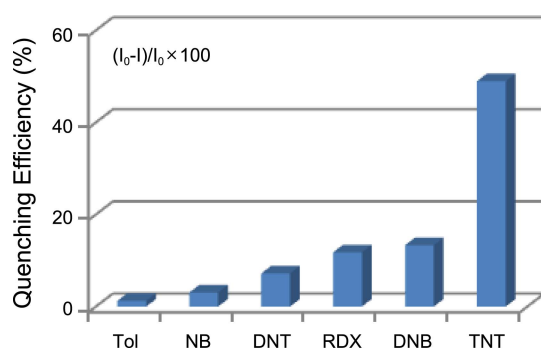


Figure 4. Quenching efficiency (reduction in fluorescence intensity) observed upon the addition of guest molecules. **4** (1.55 μM)/guest = 1:1 in water containing 1% acetone; excitation at 345 nm. RDX = 1,3,5-trinitroperhydro-1,3,5-triazine, NB = nitrobenzene, Tol = toluene, DNT = 2,6-dinitrotoluene, DNB = 1,3-dinitrobenzene, and TNT = 2,4,6-trinitrotoluene.

the pyrene derivatives is something ordered in the micelle. For instance, the TNT binding stoichiometry was examined in the micelle *via* a Job plot analysis, and the result clearly indicated that **5** forms a 2:1 complex with TNT (Figure S7 in ESI). As expected, dipyrrene derivative **4** formed a 1:1 complex with TNT (Figure S8 in ESI).

Once bispyrene **4** was selected as the best one in CTAB micelles, we then investigated the quenching efficiency of **4** with other aromatic compounds under the aforementioned conditions. As summarized in the results shown in Figure 4, the most electron-deficient aromatic substrate (TNT) displayed 45% quenching efficiency, even at a concentration of 1 equiv. The observed higher quenching efficiency could be due to the additional inclusion phenomenon of CTAB micelles so that the effective concentration of TNT could be higher in the micelles than in solutions. The presence of a larger number of electron-withdrawing nitro groups on the aromatic ring facilitated the formation of a stable complex with **4**. Additionally, non-aromatic species such as RDX induced detectable quenching effects as much as DNB did. These results indicate that non-aromatic explosives have considerable interactions with dipyrrene derivative **4** in the CTAB micelle.

To identify the detection limit for the analytes, a fluorescence titration was carried out at a low concentration of chemosensor **4** (155 nM). Surprisingly, the same method provided a twenty-fold smaller binding constant for TNT ($5.0 \times 10^4 \text{ M}^{-1}$) than for 1.5 μM of **4** at the same concentration of CTAB (Figure S6 in ESI). At a low concentration of **4**, a large proportion of the added TNT could be trapped in the micelles without **4**, which could dramatically reduce the binding constant of TNT. However, because of the large binding constant for TNT, the analysis conducted in the above condition (1.55 μM of **4** in 1.0 mM of CTAB) showed that this particular fluorescent chemosensor can detect < 2 ppb of TNT (the limit set by the US EPA on drinking water)¹⁴ and < 344 ppb of RDX (Figure S9 in ESI) in CTAB. In the case of **5**, the detection limit of TNT and RDX could be less than 10 ppb and 5.3 ppm, respectively (Figure S10 in

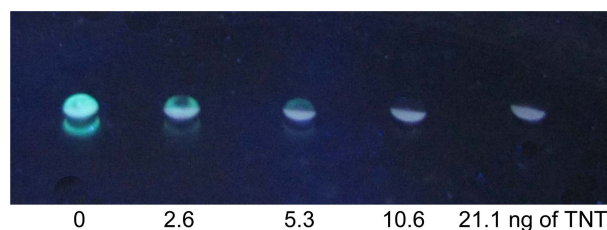


Figure 5. Changes in fluorescence observed upon the addition of **4** (15.5 μM) to various quantities of TNT spots (0 to 21.1 ng), under illumination from a laboratory hand-held UV lamp, in CTAB (1.0 mM, in water containing 1% acetone).

ESI). Further experiments also proved that receptor **4** may be used as a chemosensor under illumination from a laboratory hand-held UV lamp, using the naked eye for nitroaromatic compound detection. As shown in Figure 5, each spot was placed with various quantities of TNT on a glass plate. Then, 3 μL of **4** (15.5 μM) in CTAB was dropped onto each spot. 21.1 ng of TNT completely quenched the solution of **4**; the colored half-ellipses shown in the figure are the shadows of the drops under UV light illumination. According to these findings, the visual detection limit of TNT could be < 2.6 ng.

Conclusion

In Summary, we have shown that the relative excimer ratios (I_{ex/m_0}) of pyrene derivatives largely depend on the specificity of the micelle and the structure of the pyrene derivatives. The synthesized derivatives were found to bind to RDX effectively in CTAB micelles, although they are not without the micelle. Using these properties, the binding constants of **4** were increased by up to $1.0 \times 10^6 \text{ M}^{-1}$ for TNT in CTAB micelles, which allowed the detection of 2 ppb of TNT and 334 ppb of RDX by fluorescence titrations.

Acknowledgments. This research was supported by Inha University Research Grant and the Basic Science Research Program through the National Research Foundation of Korea (NRF), funded by the Ministry of Education, Science and Technology (grant no. 2013R1A1A2057508).

References

- (a) Steinfeld, J. I.; Wormhoudt, J. *Annu. Rev. Phys. Chem.* **1998**, *49*, 203. (b) Rouhi, A. M. *Chem. Eng. News* **1997**, *75*, 14. (c) Yinon, J. *Anal. Chem.* **2003**, *75*, 99A.
- (a) Moore, D. S. *Rev. Sci. Instrum.* **2004**, *75*, 2499. (b) Czarnik, A. W. *Nature* **1998**, *394*, 417. (c) Hakansson, K. R.; Coorey, V.; Zubarev, R. A.; Talrose, V. L.; Hakansson, P. J. *Mass Spectrom.* **2000**, *35*, 337. (d) Sylvia, J. M.; Janni, J. A.; Kleinand, J. D.; Spencer, K. M. *Anal. Chem.* **2000**, *72*, 5834.
- (a) Madhu, S.; Bandela, A.; Ravikanth, M. *RSC Adv.* **2014**, *4*, 7120. (b) Kim, S. K.; Lim, J. M.; Pradhan, T.; Jung, H. S.; Lynch, V. M.; Kim, J. S.; Kim, D.; Sessler, J. L. *J. Am. Chem. Soc.* **2013**, *136*, 495. (c) Venkatramaiah, N.; Kumar, S.; Patil, S. *Chem. Commun.* **2012**, 5007. (d) Zhang, S. J.; Ding, L. P.; Lu, F. T.; Liu, T. H.; Fang, Y. *Spectrochim. Acta A* **2012**, *97*, 31. (e) Wang, Y.; La, A.; Ding, Y.; Liu, Y. X.; Lei, Y. *Adv. Funct. Mater.* **2012**, *22*, 3547. (f) Shanmugaraju, S.; Joshi, S. A.; Mukherjee, P. S. *Mater.*

- Chem.* **2011**, *21*, 9130. (g) Lee, Y. H.; Liu, H.; Lee, J. Y.; Kim, S. H.; Kim, S. K.; Sessler, J. L.; Kim, Y.; Kim, J. S. *Chem. Eur. J.* **2010**, *16*, 5818. (h) Zhang, S. J.; Lu, F. T.; Gao, L. N.; Ding, L. P.; Fang, Y. *Langmuir* **2007**, *23*, 1584.
4. For recent review papers, see: Salinas, Y.; Martinez-Manez, R.; Marcos, M. D.; Sancenon, F.; Costero, A. M.; Parra, M.; Gil, S. *Chem. Soc. Rev.* **2012**, *41*, 1261.
 5. Goodpaster, J. V.; McGuffin, V. L. *Anal. Chem.* **2001**, *73*, 2004.
 6. (a) Andrew, T. L.; Swager, T. M. *J. Org. Chem.* **2011**, *76*, 2976.
(b) Andrew, T. L.; Swager, T. M. *J. Am. Chem. Soc.* **2007**, *129*, 7254.
 7. Freeman, R.; Willner, I. *Nano Lett.* **2009**, *9*, 322.
 8. Freeman, R.; Finder, T.; Bahshi, L.; Gill, R.; Willner, I. *Adv. Mater.* **2012**, *24*, 6416.
 9. Kim, S.-B.; Lee, E.-B.; Choi, J.-H.; Cho, D.-G. *Tetrahedron* **2013**, *69*, 4652.
 10. Hughes, A. D.; Glenn, I. C.; Patrick, A. D.; Ellington, A.; Anslyn, E. V. *Chem. Eur. J.* **2008**, *14*, 1822.
 11. Ingale, S. A. Seela, F. *J. Org. Chem.* **2012**, *77*, 9352.
 12. For CMC and Aggregation Number of Each Micelle, see: Caligur, V. *BioFiles* **2008**, *3*, 13.
 13. Ipe, B. I.; Thomas, K. G. *J. Phy. Chem. B* **2004**, *108*, 13265.
 14. US Department of Health and Human Services, Public Health Service, Agency for Toxic Substances and Disease Registry, 1995.
-